Critical Design Report

Preston Gomersall, Ben Arena, Daniel Johnson, and Ryan Banh

Table of Contents

List of Tables and Figures

Executive Summary

As the aerospace industry continues to evolve, there is a growing demand for vertical takeoff and landing (VTOL) aircrafts in both urban and military settings. In congested cities like Los Angeles and our home town of San Diego, urban air mobility (UAM) and regional air mobility (RAM) aircrafts are increasingly needed to meet transportation demands. Meanwhile, military missions often require the ability to quickly and safely transport soldiers or cargo from unprepared landing sites, making VTOL an essential feature for military aircrafts. However, current VTOL military aircrafts face challenges such as producing excessive downwash during takeoff and landing and traveling at slow speeds. To tackle these issues, our team project focuses on creating a military aircraft with advanced VTOL capabilities that can also travel at high speeds with minimal downwash.

Our team's aircraft design was created with the Vertical Flight Society (VFS) competition guidelines in mind. These guidelines required that the aircraft have VTOL capabilities, a cruise speed of 833 km/h at an altitude of 6096 m, and the ability to carry a payload of 2712 kg in a 1.98 m × 2.43 m × 9.14 m space. Additionally, the mission radius was set at 926 km, and there was an emphasis on minimizing downwash during VTOL operations. Other notable aircraft requirements are listed in Tables 1 and 2.

In addition to providing general standards, the VFS guidelines also outline a specific mission profile that the VTOL aircraft must be capable of performing, as detailed in Table 3 and Figure 1. This comprehensive mission profile includes tasks such as Hover In Ground Effect (HIGE), Hover Out of Ground Effect (HOGE), cruising, climbing, and more.

Although the competition focused on designing an aircraft that would be useful for the military, our team saw potential for a civilian market as well. With the ability to convert the cargo space to passenger seating, our aircraft could serve in the regional air mobility domain. However, the primary market for our aircraft design remains the military.

As we considered competitors in the military aircraft market, we noted existing VTOL aircraft such as the V-22 Osprey and heavy-lift helicopters like the CH-47 Chinook. There are also newer aircraft under development such as the V-280 Valor, which is capable of VTOL flight. However, our team's design provides a unique advantage in that it can carry a payload, take off and land vertically, and achieve fast cruise speeds that are comparable to traditional airplanes. By meeting the VFS competition guidelines and addressing these key market needs, our aircraft design stands out as a strong contender in the military aircraft market.

Requirements and Mission

Table 1: *Aircraft Requirements*

Crew	3 people, 250 lbs each
Limit Load Factor	3.5g

Weight Contingency	5%
Landing Gear Sink Speed	3 m/s @ ⅔ rotor lift

Table 2: *Mission Requirements*

Mission Parameters	Value (Imperial)	Value (SI)
Payload Weight	5,000 lbs	2,268 kg
Mission Equipment Package	1,000 lbs	453.592 kg
Cargo Bay Dimensions	6.5 × 8 × 30 ft	1.98 × 2.43 × 9.14 m
Cruise Speed	450 KTAS	833.4 km/hr
Minimum Cruise Height	20000 ft	6,096 m
Mission Radius	500 nmi	926 km

Table 3: *Mission Profile*

Section	Time [min]	Speed [km/hr]	Distance [km]	Description
Flight idle	10	0	0	10 minute flight idle
HIGE	2	0	0	2-min Hover In Ground Effect (HIGE) takeoff
Climb	6.35	400	42.33	Cruise-climb at best climb speed (VBROC) where range credit may be taken for the total Radius of Action (ROA) in Segments 4 and 6
Cruise	56.95	833	790.67	Cruise 450 nm (833 km/h) at be no less than 20,000 ft (6,096 m) ISA conditions or best cruise altitude at the best range speed (VBR) or no less than 450 KTAS (833 km/hr)
Descent	4.27	400	(28.47)	Descend to 2,000 ft MSL 85°F (no range credit may be taken)
Penetration	13.89	400	92.6	50 nm (92.6 km) of low-altitude, high-speed penetration
HOGE	2	0	0	2-min mid-mission Landing Zone (LZ) Hover Out of Ground Effect (HOGE) at Mid-Mission Gross Weight

				(MMGW). Segments 3-6 are repeated, followed by a 2 min HOGE landing segment. Fuel/Energy reserves shall be 20 min at VBR and 2k/85°F.
Total*	180.92	–	1851.2**	(*Total include the repeats) (**Descent range not included in total range)

Figure 1: *Mission Profile*

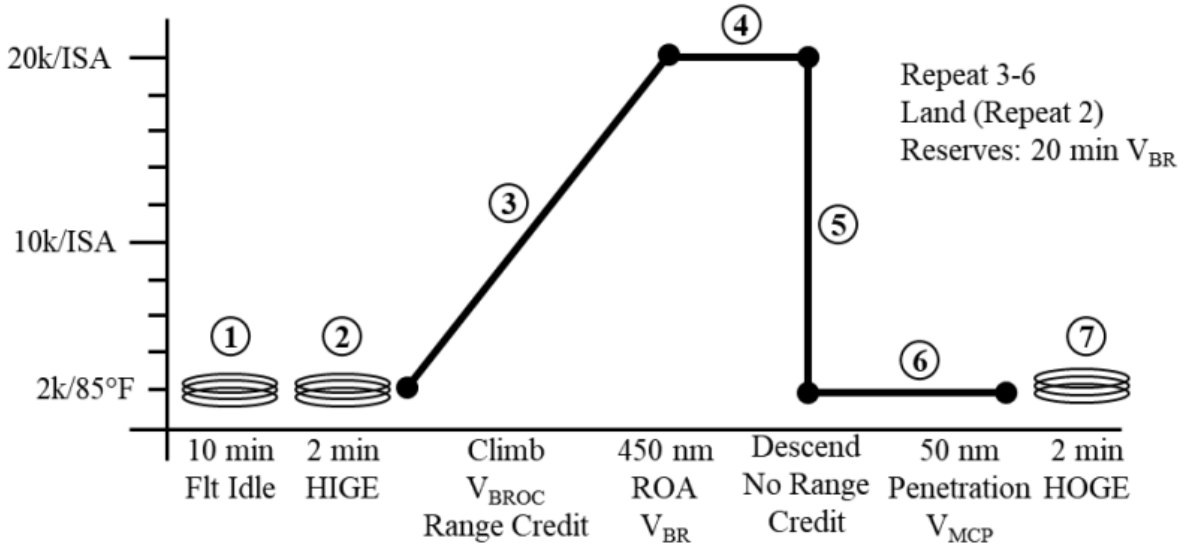

Configuration

The aircraft and mission requirements forced us to take in many considerations when deciding our aircraft configuration. Our aircraft must complete a VTOL operation while at the same time achieving a high cruising speed. Fixed rotors were not considered for our design because they would produce too much drag during cruise flight, where they would be unused. As a result, the first configuration decision that needed to be made was whether to use a tilt-rotor design or a tilt-wing design.

Ultimately, a tilt-rotor design was decided upon because the wings remain horizontal in a tilt-rotor aircraft, which allows the aircraft to generate lift through horizontal motion even before the rotors have rotated completely. Additionally, the wings would not have to be as complex, as the wings can remain fixed to the fuselage and not have to be designed to be able to rotate.

The second configuration decision that we made was regarding the propulsion system. The VFS competition specifies that the downwash during VTOL operations should be minimized, therefore large helicopter-like rotors were decided upon for the tilt-rotors. However, because of the desired high cruise speed of 833 km/h, an airscrew for propulsion during cruise flight was considered to be inadequate. Instead of receiving horizontal thrust through its

tilt-rotors, it was found that it was better to generate thrust through two turbofans. In order to avoid hazardous situations to ground crew during VTOL, and to avoid the ingestion of foreign object debris into the turbofans when hovering close to the ground, the engines must be aft-mounted and situated high above the ground.

For the tilt-rotors, we had to decide whether or not they would be powered by mechanically-linked turboshaft engines or by electric motors. Because the weight of heavy turboshaft engines acting on the wingtips would require much more structural support, and because having two additional, rotating engines on the aircraft would increase the complexity and maintenance required significantly, it was decided that electrically-driven rotors would be a more ideal solution. With electric motors driving the rotors, it was then necessary to choose whether or not their energy source would be derived from batteries or through a turbo-electric powertrain.

Through careful analysis of battery technology and the power required when the aircraft is hovering, it was concluded that even with optimistic forecasts for future battery densities, it would not be possible to power the rotors for an extended period of time before the batteries were drained. This would be unsafe and would severely limit the performance of the aircraft. As a result, it was decided that, rather than a battery, a turboshaft engine connected to a generator would power both of the electric motors. Being a single engine and not having to rotate with the rotors, it would be far simpler and easier to perform maintenance. Additionally, current turboshaft engines, weighing the same amount as the batteries used in the first analysis, are capable of producing the power output required.

Because of the separation of VTOL and horizontal propulsion, each can be optimized for their own purposes. The turbofans will effectively generate thrust to achieve the high cruising speed while the large, helicopter-like rotors will allow for effective VTOL operations with reduced downwash. However, an issue that is introduced with the separation of horizontal and vertical propulsion systems is that they can interfere with each other's operations. For example, during cruise flight, the tilt-rotor's rotor blades will create a large amount of drag while contributing nothing to propulsion. During VTOL operations, the turbofans, which will remain powered on, will produce forward motion while the aircraft is expected to hover in place. The VTOL and Cruise Flight Operations are depicted in Figure 2.

The solution for this is to "disable" one of the propulsion systems when the other is being used. In cruise flight, the rotor blades can be folded back against the tilt-rotor nacelles, reducing the drag they generate (displayed in Figure 2 and 3). During VTOL mode, the aft-mounted turbofans can be set to idle power and their remaining thrust negated using thrust deflectors or a modified form of thrust reversers. It is necessary to negate the thrust rather than to stop and start the turbofans mid-flight because it may introduce issues having to go through engine startup procedures while flying. Additionally, because of the expected military use of this aircraft along with the mission profile expecting a quick transition between hovering and horizontal flight, it is important that the pilot not need to wait for the engines to start up before transitioning. This is a

waste of fuel, but if fuel consumption is a concern, the turbofans could also be shut down and started up again instead.

Figure 2: *VTOL and Cruise Configurations*

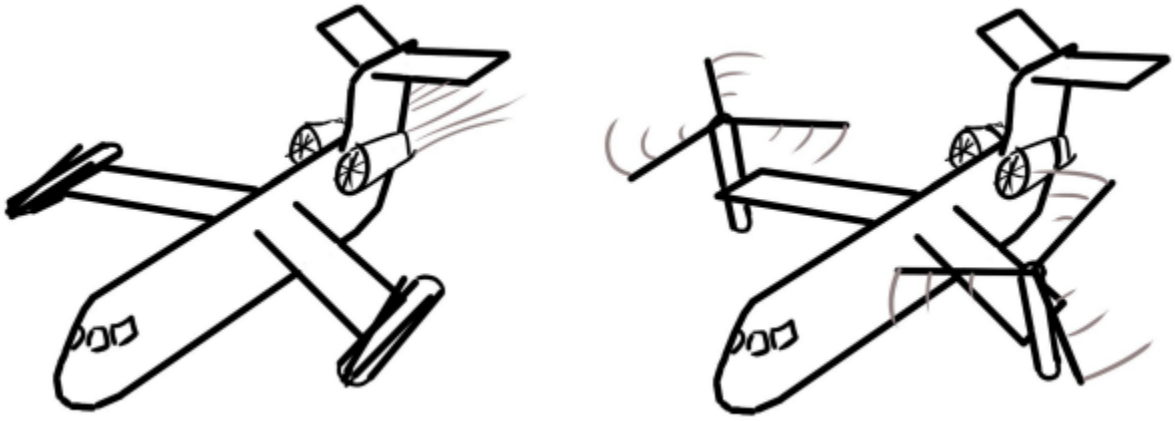

Cruise Flight Operation *VTOL Operation*

Multiple decisions had to be made for the lifting surfaces of the aircraft as well. For the wing, because of the high cruise speed approaching transonic speeds, it was determined that a swept wing should be used to reduce the wave drag. As such, we had to decide whether or not to use a back-swept wing or a forward-swept wing. A back-swept wing would be more stable than a forward swept wing, both structurally and aerodynamically. Despite this, the simple fact that tilt-rotor propellers would collide with a back-swept wing when tilting forward forced us to consider a forward-swept wing of 5°. A taper ratio of 0.5 was decided for aerodynamic performance, and the wing was mounted high with an anhedral angle. By keeping the wings high off of the ground, it increases ground clearance and reduces the downwash felt on the ground, which is important to consider for the intended use-case of this aircraft.

For the empennage, we had to decide between a traditional horizontal stabilizer and a T-tail form. A traditional horizontal stabilizer would receive airflow even during high angles of attack while a T-tail would have its airflow disturbed by the wing below it. Additionally, a T-tail requires more structural support. However, a traditional horizontal stabilizer would interfere with the aft-mounted engines, so a T-tail configuration was superior in this situation.

Figure 3: *Propeller Folding Design*

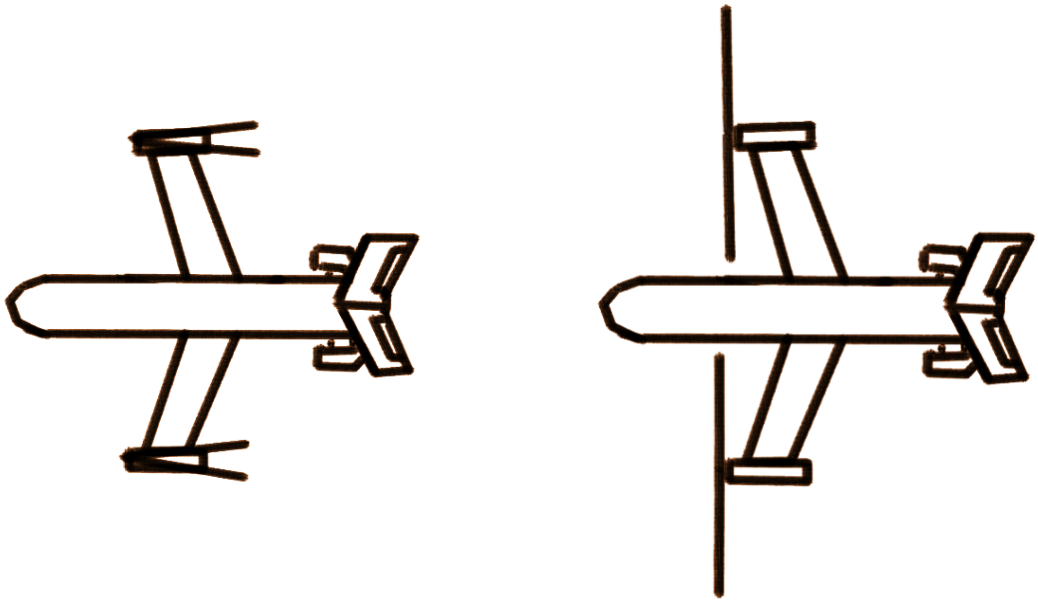

Rotors Stowed *Rotors Deployed*

With the wing and empennage of a traditional airplane, the control surfaces during cruise flight allow the aircraft to be controlled like a regular airplane. During VTOL operations, for ease of control, the only control will be provided through the tilt-rotors. The turbofans will have their thrust nullified so that only the rotors have an effect on the control. To control yaw, the rotors will tilt slightly in opposite directions, so the tiltrotors will be required to have a range of motion greater than 90°. Like a helicopter, pitch would be controlled through cyclic pitch control. The rotors will have to be counter-rotating to avoid having a torque imparted on the airframe that generates undesirable yaw, and since they need to both rotate at the same speed to achieve this, roll control will be provided by collective pitch control on either rotor. Because cyclic pitch control is already required, collective pitch control can be implemented for no additional cost in complexity.

Sizing

To determine the appropriate sizing for our aircraft, we conducted research and analysis based on the reference aircrafts of the V-280 Valor and the V-22 Osprey. While the V-280 Valor closely matched our desired size and speed, there was a lack of information on the aircraft, as it is still in production. The V-22 Osprey was able to provide us with valuable initial specifications for climb speed, stall speed, crew weight, fuel weight, and payload weight fractions, which we used to compare and refine our calculations.

Using historical specifications and our own requirements, we created a sizing plot in Matlab shown in Figure 4, which helped us to determine thrust loading and wing loading. We

then developed a Matlab code that incorporated the Breguet range equation, allowing us to calculate a feasible fuel weight fraction, takeoff weight, thrust needed, and total mass of fuel required for our mission. We repeated this process until our values aligned with our expectations and were reasonable. Our final values compare favorably to those of the V-22 Osprey, and are summarized in the weight fractions, wing loading, and thrust loading table below (Table 4).

Table 4: *Sizing*

Takeoff Weight	17031 kg
Empty Weight Fraction	0.6036
Fuel Weight Fraction	0.2183
Crew Weight Fraction	0.01997
Payload Weight Fraction	0.1598
Thrust Loading (T/W)	0.2213
Weight Loading (W/S)	650

Figure 4: *Sizing Plot*

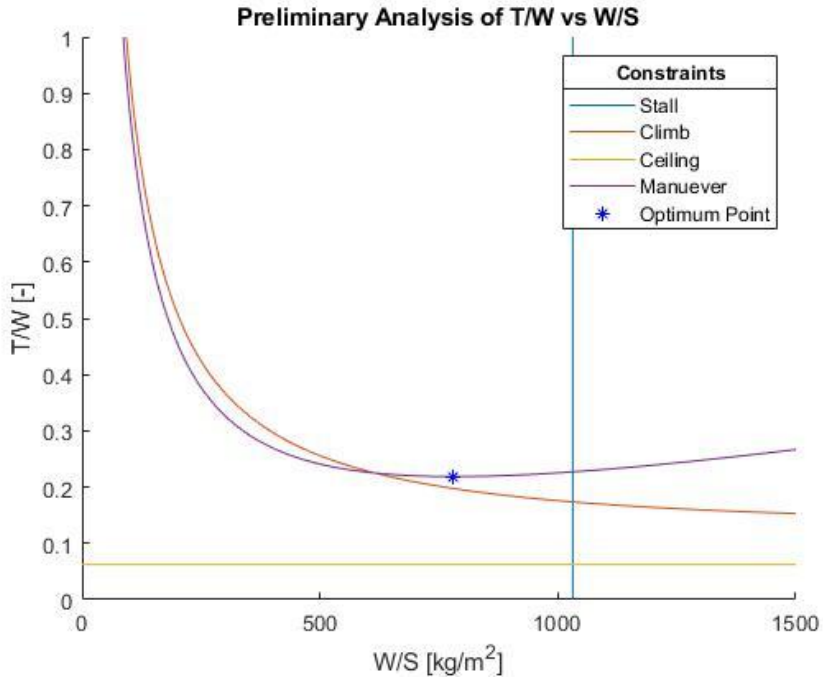

The next step in the design process was to determine whether our aircraft was capable of flying the range we needed based on the fuel weight fraction, thrust weight fraction, and everything else in Table 4. We then plotted a payload diagram shown in Figure 5, which shows

our aircraft design is capable of flying the full range specified by the VFS competition with the full payload specified. The fuel tank has 25% more capacity than a full mission requires. As the fuel increases beyond that amount, the payload weight must decrease in order to keep the take-off weight from exceeding the maximum take-off weight. Once the fuel tank is at full capacity, no more fuel can be added, but the range can still be extended by decreasing the weight of the payload, yielding a lighter aircraft and thus further range.

Figure 5*: Payload Range Diagram A*

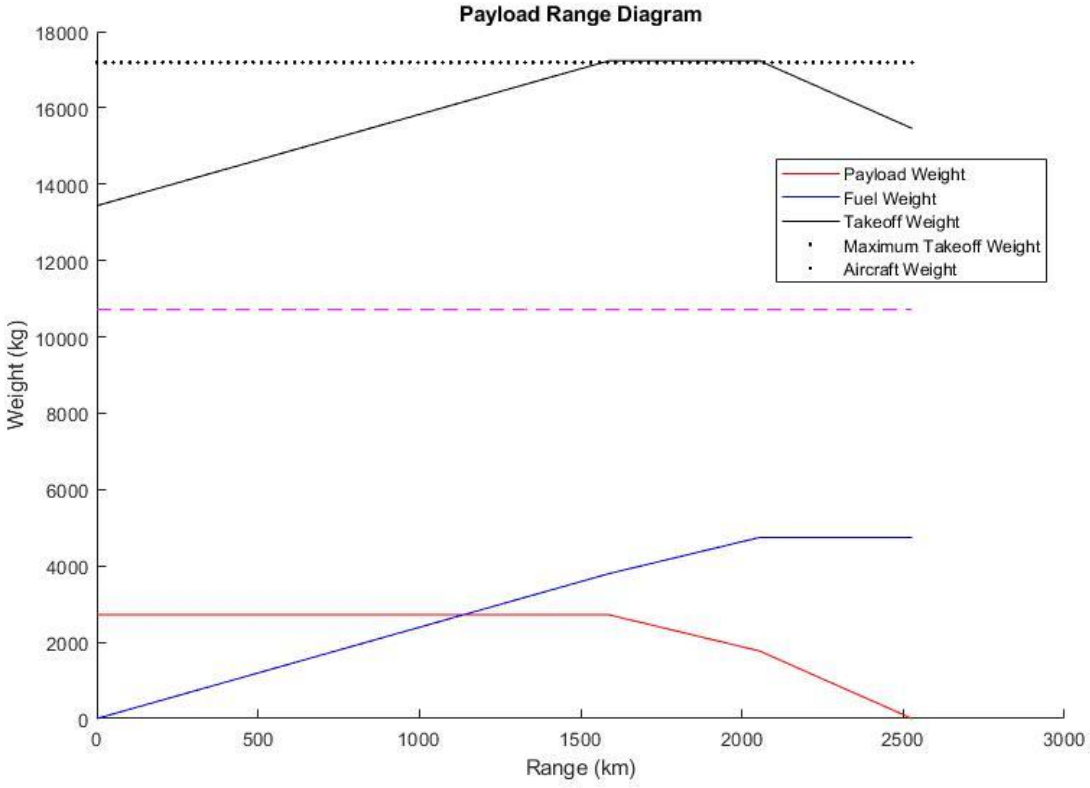

Figure 6: *Payload Range Diagram B*

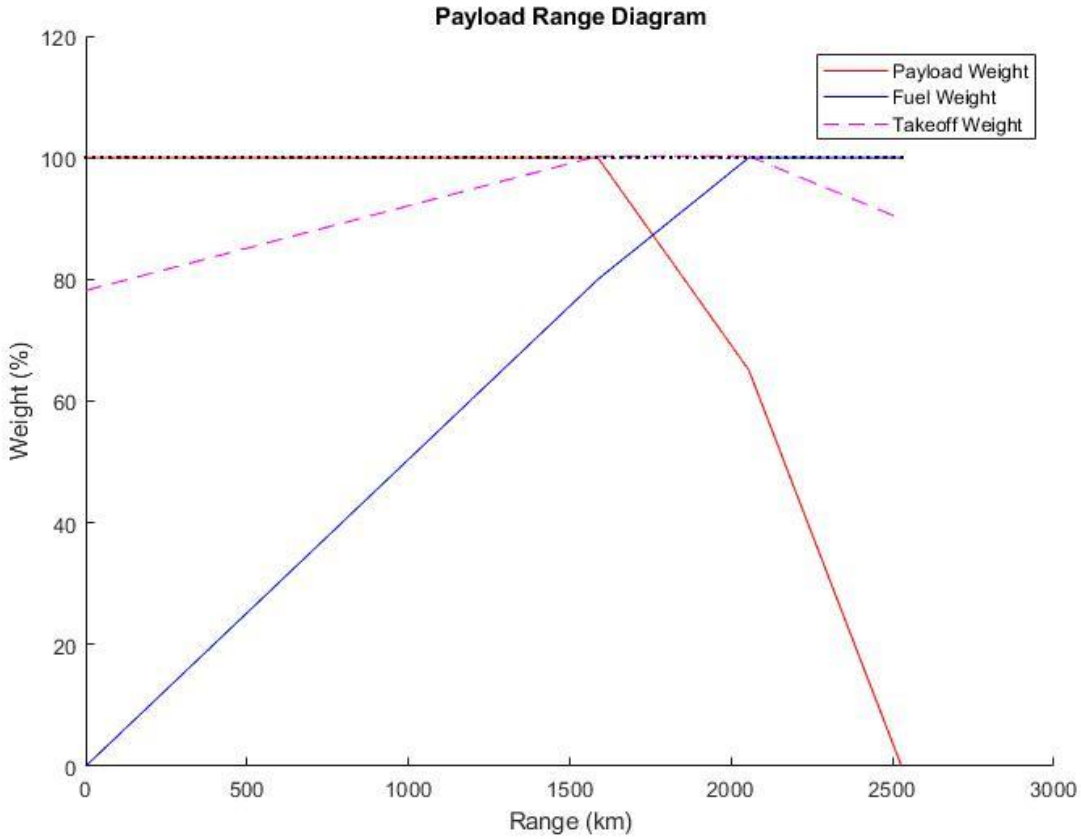

The payload range diagram above shows this dynamic as a percentage of its maximum weight rather than total weight. As can be seen, there is a tradeoff between payload weight and range once the fuel reaches the point where the full payload can be carried its required range. This shows that despite the rated range of the aircraft, it applies to the full payload capacity, and the aircraft can actually travel significantly further if one decreases the payload carried onboard.

Propulsion

The configuration is a turbo-electric system. The VTOL rotors will be electrically powered with motors, with the electricity being generated by a turboshaft engine connected to a generator as shown in Figure 6. This configuration was chosen because the VTOL rotors are only used for a small fraction of the flight, meaning that there would be two engines that are not used as often yet still need to be maintained and designed to articulate as it is a tiltrotor design. A single non-moving turboshaft engine with electric motors is simpler to design and maintain. Batteries were not used because battery technology, even in the future, will not be able to provide the power necessary to operate in VTOL configuration for an extended period of time.

Figure 7: *Propulsion System Diagram*

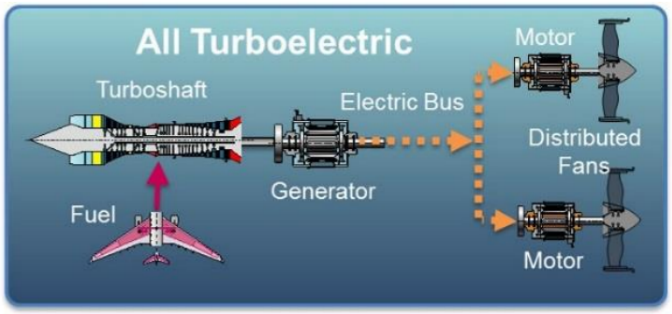

For our engines we chose to mount two PW306b turbofans on the rear of the plane. According to our calculations we need a maximum thrust of approximately 19.16 kN per engine in order to reach the goal speed of 833 km/hour. The PW306b turbofans displayed in Figure 7 can more than accommodate our needs with a maximum thrust of 21.13 kN each. We chose a turbofan over other options because of the lower fuel consumption when compared to a turbojet, the lack of feasibility of a propeller plane working at a height of over 6000 meters, and we approach but to not cross into the area of transonic speed with a Mach number of 0.7320 at cruise.

Figure 8: *PW306B Turbofan*

PW306B Turbofan	Value
Overall Length	1888 mm
Overall Height	1138 mm
Overall	965.2 mm
Overall Diameter	1138mm
Thrust, Maximum Continuous	26910 N
Interturbine Temperature Continueous	920 C
Low Pressure Rotor N1 rpm	11138 rpm
High Pressure Rotor N2 rpm	28277 rpm
Cruise Thrust	5,030 N

The electric motors require a power source, and the battery density required to store the power is not realistic with today's technology. Even when accounting for battery advancements in the future, it is still an infeasible configuration, as we would need a battery density increase from the present day maximum of around 170 Wh/kg to a value of 1,000 Wh/kg to keep the battery weight within 500 kg.

However, modern turboshaft engines are already capable of achieving the required power output while weighing 500 kg. General Electric's T408 turboshaft engine, for example, weighs 500 kg while being capable of producing 5,600 kW of shaft power. Thus, a turbo-electric system for powering the VTOL rotors is the ideal solution in this case.

Next, our team decided what motor to use for our rotor system. The Magni650 shown below is one of the best electric motors suited for flight on the market today and, in May of 2020, was able to power the largest electric aircraft to ever take flight—a modified Cessna Grand Caravan 208B. This motor, however, is only capable of outputting 640 kW, approximately one-fourth of what is required in our design. It can be reasonably assumed that electric motors will only improve in performance in the following years. However, if electric motors are still unable to produce the power output required by the 2030s, then it is possible to have multiple motors powering one rotor, similar to how some helicopters have two turboshaft engines simultaneously providing power to their rotor.

Figure 9: *Magni650 Motor*

Description	Value
Motor Type	Electric
Power	640 kW

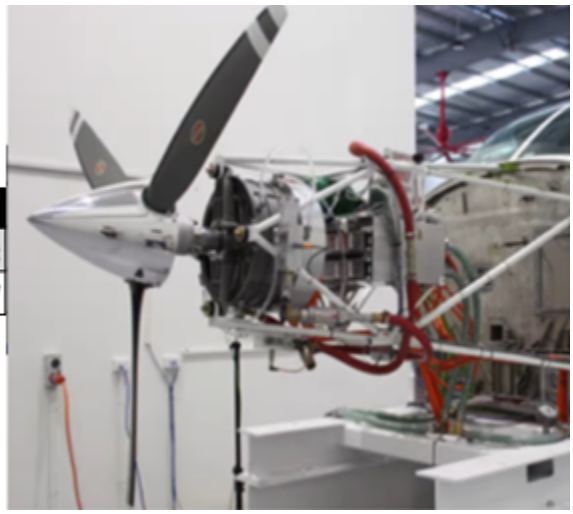

Aerodynamics

After careful consideration, we selected the RAE 2822 Airfoil as the optimal choice for our aircraft's needs. Our sizing parameters and aerodynamic requirements dictated that we needed an airfoil capable of achieving a lift-to-drag ratio of at least 16 during cruise conditions, designed for transonic flow, and capable of handling high Reynolds numbers. Based on the drag polar graph displayed below in Figure 9, we determined that the RAE 2822 Airfoil shown below was the best option for us to achieve this C_l/C_d ratio.

In addition to its aerodynamic capabilities, we needed an airfoil that was thick enough to accommodate the fuel necessary for our flight and could withstand the stress imposed by our forward swept wings. However, given our aircraft's high-speed performance requirements, we also needed an airfoil that would minimize drag during flight. To achieve this balance, we decided to use a thin airfoil that is still thick enough to accommodate our fuel requirements.

To optimize our aircraft's performance, we made several design choices regarding the wing's twist angle, taper ratio, and forward sweep angle. We added a twist angle of 3 degrees from the root to the tip, which helps to prevent stall at the root of the wing. By doing this, we can

ensure that the wing stalls in a controlled manner, reducing the risk of sudden and unpredictable stall behavior.

In selecting a taper ratio of 0.5, we considered multiple factors. We wanted to ensure that there is enough space on the root tip of the plane for mounting the propellers and motors, while minimizing the amount of downwash created by the taper ratio. This allowed us to maximize lift and control while reducing the potential for turbulence and drag.

Finally, we decided on a forward sweep angle of 5 degrees, which helps to minimize the onset of wave drag while still allowing the propellers to function without interfering with the planform. This configuration provides an optimal balance between aerodynamic performance and functionality, enabling us to achieve maximum speed and efficiency while maintaining excellent control and stability.

Figure 10: *RAE 2822 Airfoil*

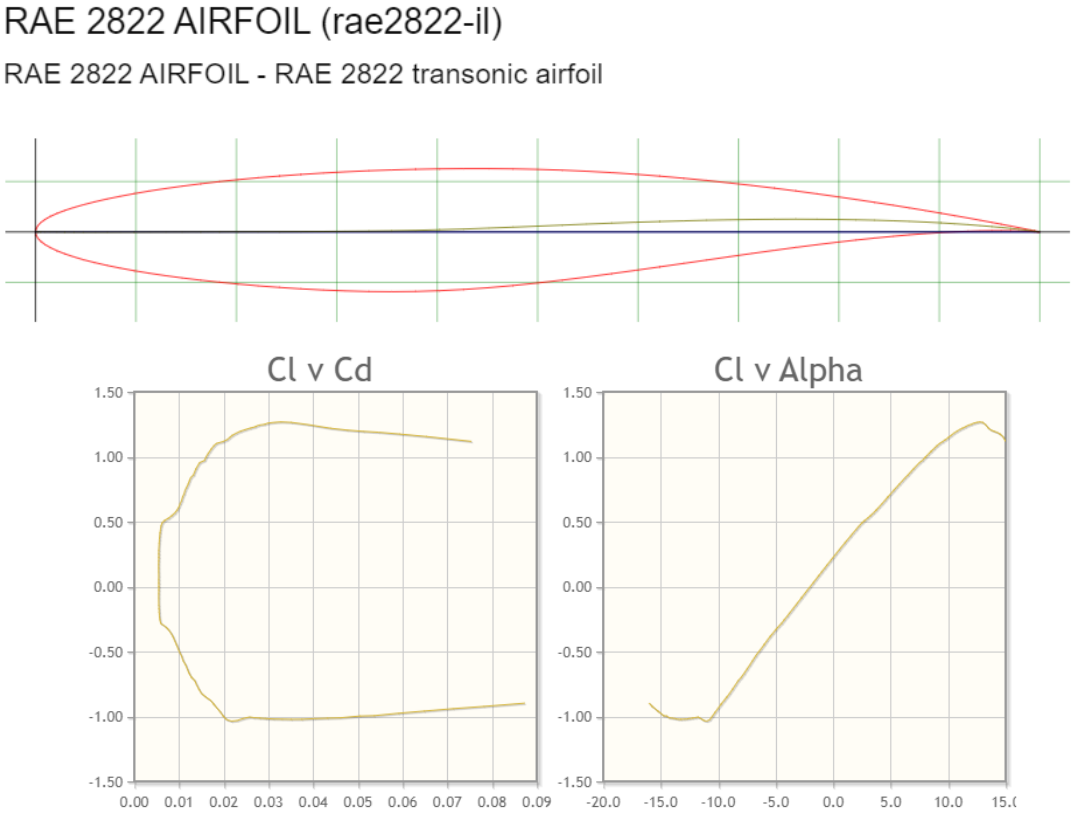

By utilizing the equations presented in our class and textbook, we were able to precisely calculate the aerodynamic coefficients required to design our aircraft's geometry. These coefficients, which are presented in Table 5, provide a comprehensive overview of the aircraft's aerodynamic characteristics during cruise flight.

Our calculations allowed us to determine the optimal wingspan, as well as the ideal location of various aircraft components in relation to one another. This enabled us to strategically

position key components such as the landing gear and aft-mounted engines for maximum effectiveness.

Overall, these calculations provided us with the critical information we needed to design an aircraft that is both highly efficient and highly effective in achieving our desired performance parameters.

Table 5: *Aerodynamic Values*

C_{D0}	0.0150
C_{Dw}	0.5929
C_D	0.0836
$C_{L,cruise}$	0.3435
L/D	20.4934
AR	7
Span	13.64 m
X_{cg}	8.3151 m (9 % of the chord)
X_{np}	8.5713 m (22 % of chord)
Static Margin	13.15%

The next thing to consider was our tail design. To determine tail sizing, we used the typical values for tail volume coefficients (C_{HT} and C_{VT}) and worked backwards from our design, such as our wing sizing and tail placement, to determine both vertical and horizontal tail area. This area was used then to determine the root chord of the tail components and then to size the elevator and rudder. Similarly the design of our ailerons and flaps will use typical sizing based on our class of aircraft. Our tail and control surface sizing is given in Table 6 below:

Table 6: *Tail and Control Surface Sizing*

	Value	Percent of Reference
C_{HT} (horizontal tail)	1.00	-
C_{VT} (vertical tail)	.09	-
AR (horizontal tail)	3.5	-
AR (vertical tail)	1.7	-

S (horizontal tail)	6.32 m^2	-
S (vertical tail)	3.9827 m^2	-
Horizontal Tail Root Chord	2.0676 m	-
Vertical Tail Root Chord	3.7377 m	-
Taper ratio (Vertical and Horizontal)	.5	-
Elevator Chord Length	.5169 m	25% of tail chord
Rudder Chord Length	.7535 m	32% of vertical tail chord
Aileron/Flap Chord	.4287 m	22% of wing chord
Total Aileron Span	5.456 m	40% of wing span
Total Flap Span	6.1380 m	45% of wing span

These values are derived from the Daniel Raymer textbook charts, which are based on reference aircraft in our class. For our tail design, we chose the NACA-0009 airfoil, which is a good choice because for aircraft symmetric airfoils are favorable in the tails as they allow for more control authority using our control surfaces. With our tail sized, we can get the aerodynamic center of our aircraft which comes out to X_{np} = 28% of the wing chord. This coupled with the X_{cg} = 14.5% of the wing chord gives static margin of SM = 13.54%. Which is a good value for our class of aircraft. This makes the aircraft statically stable while also trimming the aircraft during disturbances that cause the plane to nose up. This is important so that in stall, our aircraft naturally noses down rather than up. This is a similar reason as to why the aspect ratio for the horizontal stabilizer is much smaller than that of the wing. Lower aspect ratio causes the tail to stall later than the wing, this allows for continued elevator control in stall so that a pilot can pitch the nose down if needed. The flap is sized to be as large as possible to decrease stall velocity during takeoff and our ailerons are sized to allow for greatest control.

Propeller Design

For the VTOL rotor blades, we used the Hughes Helicopters HH-02 rotorcraft airfoil. This airfoil has promising C_l and C_d data which fit well within many of our constraints. A root twit of 4.8 degrees was added in order to distribute the lift generated across the length of the blade more evenly. The diameter of the blades are very large (about 45% of the wingspan) in order to generate the most possible lift while also maintaining a wingtip speed below Mach 1. Other key data is displayed below in Figure 11 and Table 7.

Figure 11: *Hughes Helicopters HH-02 Airfoil*

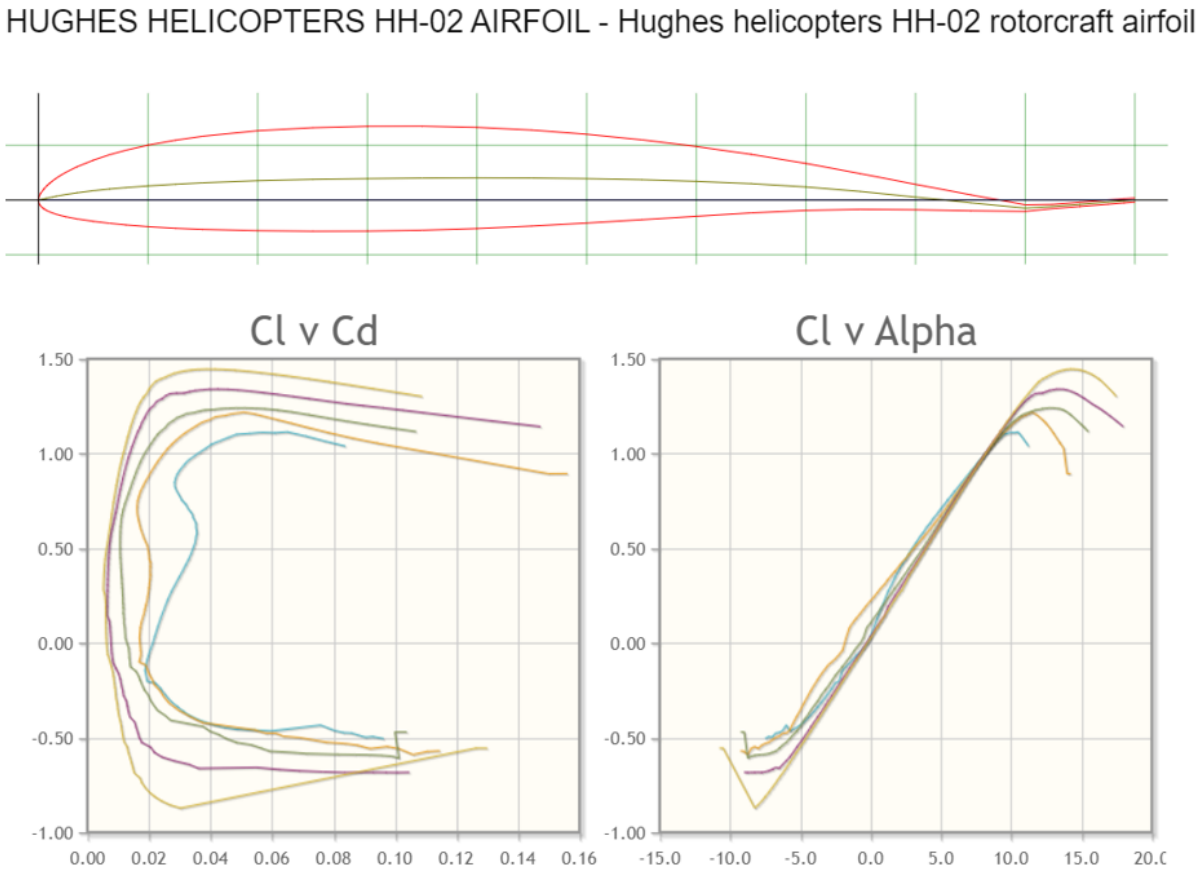

Table 7: *Propeller Data*

Description	Value
Disk Loading	229.69 (*N/m^2*)
Efficiency	0.43
C,t	0.01511
Rotational Speed	308.7 (*m/s*)
Advance Ratio	0.63
Diameter	6.73 (m)
Root Twist	4.8 (degrees)
Blade Solidity	0.15
T/C Ratio	0.118

Dynamic Stability

The aircraft we are designing for the VFS competition requires both dynamic and static stability during vertical takeoff and landing (VTOL) as well as cruise flight. As this is not an aircraft designed for combat and its primary purpose is to carry cargo—high maneuverability is not a priority.

We chose to base our wing design off of the V-22 Osprey, which uses an anhedral wing with small winglets at the end. We will adopt this idea and use an anhedral angle with winglets and place the wings high on the fuselage. This design increases maneuverability while providing good stability during a banking maneuver. Additionally, high-mounted wings bring the rotors higher off of the ground, decreasing downwash, as well as increasing ground clearance for ground crew.

The forward sweep of the aircraft also provides extra stability by moving the center of pressure closer to the aerodynamic center, which reduces the aerodynamic moment about the AC and the bending moment on the wing. This also reduces the size of the tail, as less lift is needed to counteract moments about the center of gravity.

To ensure stability during cruise flight, we use standard techniques and position the aerodynamic center behind the center of gravity with a static margin of 10%. Ailerons are used for stability during rolling maneuvers, while elevators and the T-shaped tail design provide stability during pitching maneuvers. The rudder is used to control any yawing motion.

During VTOL flight, the two rotors control the stability of the aircraft. By rotating in opposite directions, they produce a yawing moment on the aircraft, and like helicopter rotors, collective pitch control and cyclic pitch control the aircraft's roll and pitch, respectively. Collective pitch control on the rotors changes the thrust produced by either rotor, providing roll control, and cyclic pitch control on the rotors allows for a pitching moment.

Weights

Our team calculated the weight values for our aircraft by utilizing equations taught in our aerospace design class and taking inspiration from the V22-Osprey. Because the Osprey shares a similar fuselage and wing design to our intended aircraft, we derived some of our weight estimates from it. However, since the Osprey is larger in size, we made necessary adjustments to the weight of our fuselage and wings to ensure proportional similarity. Additionally, the payload and cargo weights were determined based on the VFS competition specifications while fuel weight was calculated considering the aircraft's range and thrust produced by the turbofans. For the landing gear and electronics, we referred to other aircrafts that had comparable VTOL maneuvers. To arrive at our gross weight estimate, we included fudge factors for most components, keeping in mind that technology and material properties will have improved by the time our aircraft is expected to be released in the mid-2030s. These weights values are all shown in Figure 11.

Furthermore, we estimated the location of the weight distribution along the fuselage and calculated the center of gravity for the entire aircraft, which we found to be positioned 8.33 meters from the front of the fuselage. The wing was then placed slightly behind the center of gravity at x = 9 meters to ensure the aircraft remained stable during flight. This strategic placement allows the lift at the aerodynamic center to counteract any pitch up moments and maintain the desired angle of attack.

Table 8: *Distribution of Weights*

Part	Weight (kg)	Moment Arm (m)	Fudge Factor	Fudged Weight
Payload + Cargo	3060.19	12.07	1	3060.19
Wings	1603	7	0.75	1202.25
Tail	907.19	16.5	0.7	635.033
Fuselage	8870	8.5	0.6	5322
Fuel	3534	8	1	3534
Generator Weight	500	7	1	500
Landing Gear	1313	10	0.7	919.1
Electronics and Propellers	1000	6.5	0.71	710
Engines	1350	10	0.85	1147.5

Figure 12: *Distribution of Weights*

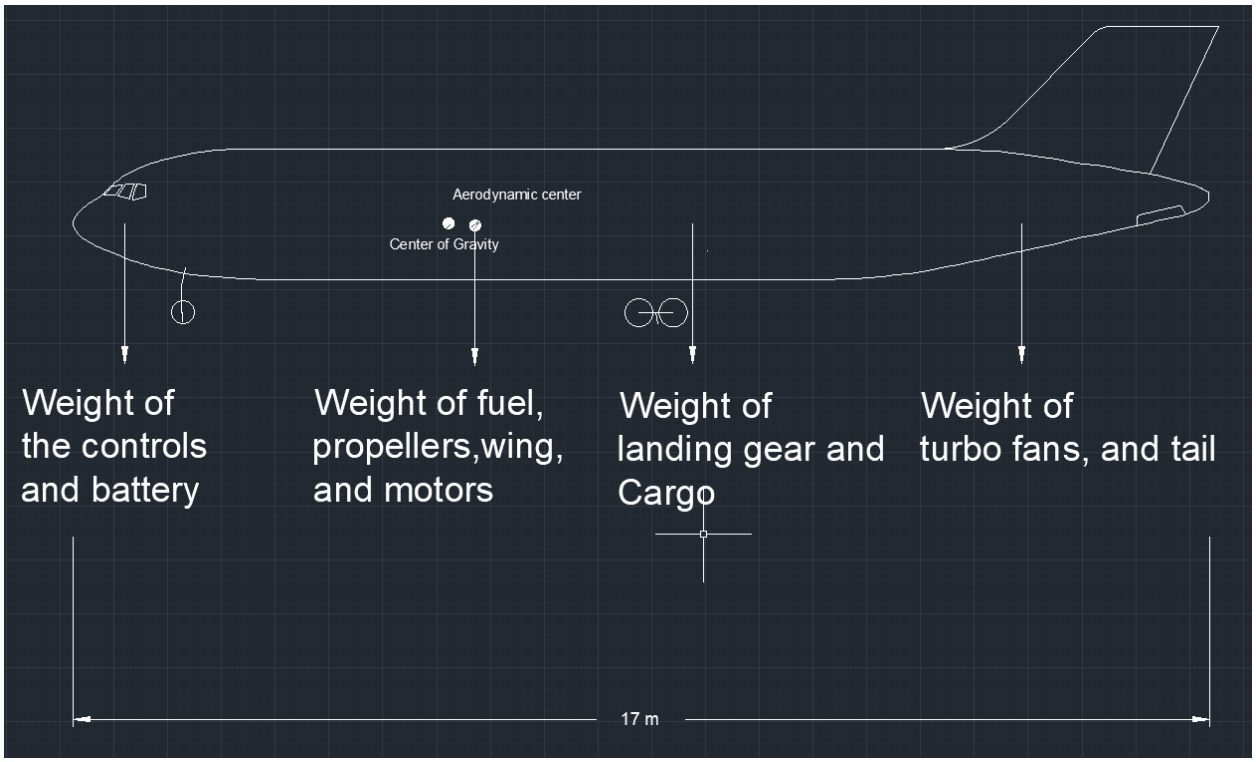

V-n Diagram

Next, we calculated the load factors of our aircraft relative to our velocity on the V-n diagram. The maximum load factor for maneuvering was provided by the VFS competition guidelines. The minimum load factor was estimated to be –1.5 based on the structural strength of the wings and aircraft. The stall velocity was calculated from our Cl_{max}, the wing area, and dynamic pressure. The cruise velocity was set by the competition guidelines. The V_{dive} was estimated based on when we determined our wings will fail from flutter. The load factors from wind gusts were calculated in the V-n diagram, shown by the red envelope. This gust envelope accounts for winds of 25 ft/s and 50 ft/s.

Figure 13: *V-n Diagram*

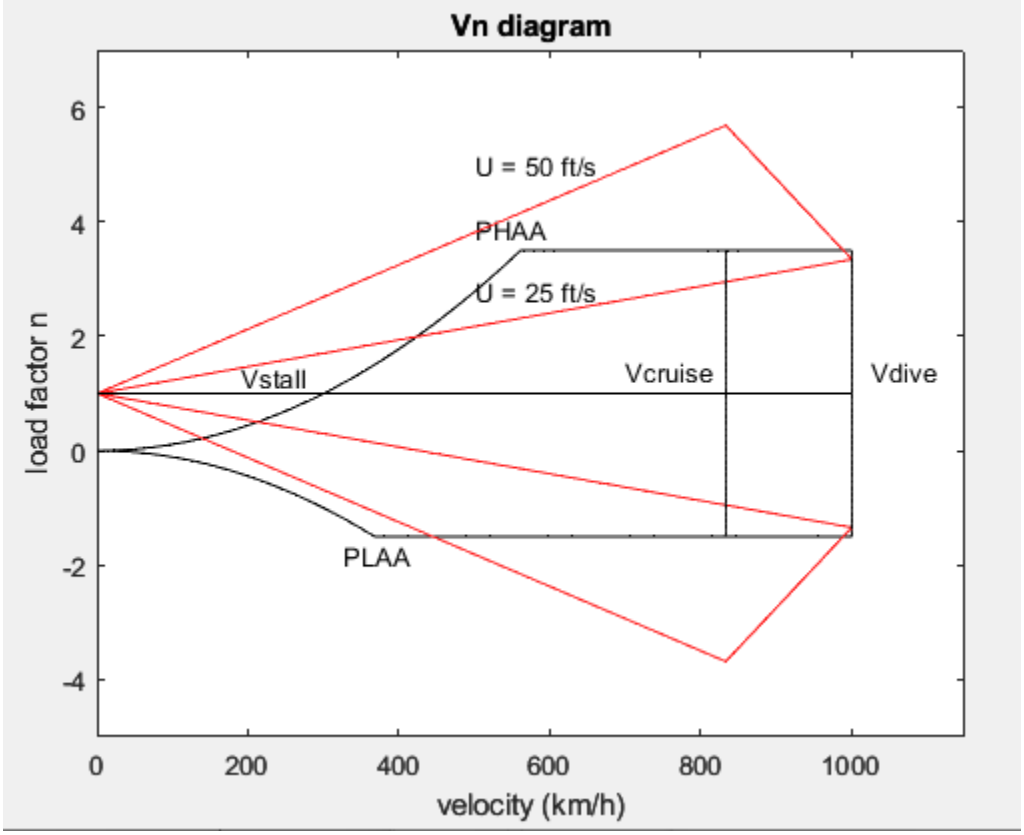

Cost

For estimating the cost of the research and development, testing and evaluation, as well as the flyaway cost of the aircraft, a lower estimate of 20 aircraft produced in five years was used. Because of the intended military usage of this aircraft, a relatively low number of aircraft is expected compared to quantities associated with commercial endeavors. Additionally, a quantity of three testing aircraft was used. To estimate the costs, equations from *Aircraft Design: A*

Conceptual Approach (Daniel) were used. Because the equations prescribed gave its values in 2012 dollars, an inflation rate of 31% was used to find the equivalent cost in 2023. Additionally, a 40% increase on the dollar amounts was applied to account for interest and contractor profit.

Table 9: *Man-Hours to Produce Aircrafts (in millions of hours)*

Engineering Hours (H_E)	6.679
Tooling Hours (H_T)	3.317
Manufacturing Hours (H_M)	5.468
Quality Control Hours (H_Q)	0.416

These man-hours were multiplied with the corresponding wrap rates of Engineering R_E = \$115, Tooling R_T = \$118, Quality Control R_Q = \$108, and Manufacturing R_M = \$98 to calculate the labor costs associated. The wrap rates include the salaries paid to the employees and the benefits, overhead, and administrative costs, serving as a good method of estimating the cost of employing workers to work these many hours. With the cost of labor found, the monetary costs themselves can be calculated.

Table 10: *Aircraft Costs (in millions of USD)*

Development Support Cost (C_D)	358.39
Flight Test Cost (C_F)	63.93
Manufacturing Materials Cost (C_M)	321.49
Engine Production Cost (C_{eng})	1.86
RDT&E + flyaway	4,031.6

The combined cost of RDT&E and flyaway cost of the aircraft amounts to just over \$4 billion. In comparison to the budget that the US military typically allocates for procurement of new aircraft, this value is appropriate and comparable to other programs.

References

[1] Vertical Flight Society. (2022). VFS 40th Annual Student Design Competition 2022-2023 Request for Proposals (RFP). Vertical Flight Society.

[2] Torenbeek, Egbert. *Synthesis of Subsonic Airplane Design*. Kluwer Academic Pub., 1990.

[3] *Bell V-280 Valor - future Long Range Assault Aircraft (FLRAA)*. Bell Flight. (n.d.). Retrieved February 17, 2023, from https://www.bellflight.com/products/bell-v-280

[4] Wikimedia Foundation. (2023, February 14). *Bell Boeing V-22 Osprey*. Wikipedia. Retrieved February 17, 2023, from https://en.wikipedia.org/wiki/Bell_Boeing_V-22_Osprey

[5] Lavars, N. (2019, October 10). *Magnix's 750-hp electric motor turns its first propellor at full bore*. New Atlas. Retrieved February 17, 2023, from https://newatlas.com/aircraft/magnixs-750-hp-electric-motor-first-propellor/

[6] Raymer Daniel, P (1999). “Aircraft Design: A Conceptual Approach”. In: AIAA Education series.

[7] *GE's T408 Turboshaft Engine*. GE Aerospace. (n.d.). Retrieved March 10, 2023, from https://www.geaerospace.com/propulsion/military/t408

[8] *Airfoil tools*. Airfoil Tools. (n.d.). Retrieved March 6, 2023, from http://airfoiltools.com/